CrystEngComm

Accepted Manuscript

ROYAL SOCIETY OF CHEMISTRY

www.rsc.org/crystengcomm

CrystEngComm

PAPER

A Solventless Mix-Bake-Wash Approach to the Facile Controlled Synthesis of Core-Shell and Alloy Ag-Cu Bimetallic Nanoparticles

Received 00th January 20xx,
Accepted 00th January 20xx

DOI: 10.1039/x0xx00000x

www.rsc.org/

Eunjin Choi,[ab] Sohee Lee[ab] and Yuanzhe Piao[*abc]

We report a solventless mix-bake-wash method for the facile controlled synthesis of Ag-Cu core-shell and alloy bimetallic nanoparticles (NPs). Small bimetallic nanomaterials were prepared by a one-step heating process using salt powder as a template. The particle structure could be controlled by tuning the annealing temperature to generate hetero-structured core-shell NPs or homogeneous alloys. The NPs' bimetallic structure and elemental analysis were characterized by HR-TEM, FE-SEM, EDX, HADDF-STEM, XRD and XPS. Whereas the as-synthesized Ag@Cu core-shell NPs consist of a core of face-centered cubic (fcc) polycrystalline Ag NPs and a shell of fcc Cu including trace amounts of copper oxides, an AgCu nanoalloy was found to comprise a single-phase NP with the same crystal structure as that of Ag, without the copper oxide species. Cyclic voltammetric measurement confirms the chemical identification of the surface species and their stability to oxidation. This synthesis approach is facile, structure-controllable, and scalable, and expected to be capable of producing other bimetallic or trimetallic nanomaterials.

Introduction

Bimetallic nanoparticles (NPs) have attracted considerable attention for their potential applications in the fields of catalysis,[1] optics,[2] magnetism,[3] and biology.[4] In many cases, these NPs have not only the distinct characteristics of both component elements, but also new and unexpected properties from alloying owing to the synergistic effect.[1e,2d,5] The preparation of bimetallic NPs has been intensively investigated for many years, and a variety of fabrication methods, including chemical reduction,[6] thermal decomposition,[7] sonochemical synthesis,[8] electrochemical deposition,[9] ion implantation,[10] and microwave-assisted synthesis,[11] have been developed. One of the goals of these various synthesis methods is to control the structure of bimetallic NPs to obtain specific structures such as core/shell, heterodimers, or alloy.[12] The precise control of not only the structure but also chemical composition, size, and atomic ordering of NPs is important to modern materials science because these factors can affect their physical and chemical properties.[2d,5,13]

Among many bimetallic NPs, Cu-based NPs incorporated with noble metals in the form of core-shell or alloy structures have a number of advantages compared to mono-element metallic NPs, such as much higher catalytic activity,[14] better antibacterial ability,[15] and the application of low-cost conductive patterns for electronic devices.[16] The preparation of Cu-based bimetallic NPs has been explored by many research groups in recent years. Park and Liu's groups fabricated raspberry-like Ag@Cu NPs via a stepwise reduction process using poly(vinylpyrrolidone) (PVP) as a stabilizer for preventing the aggregation of NPs;[6a] Ying's group showed a seed-mediated growth approach for rod-shaped AuCu nanoalloys using oleylamine (OAm) as a capping agent for shape control.[14c] Sun's group synthesized CuPd and CoPd NPs by co-reducing precursors in a solvent and a reducing agent of OAm and a stabilizer of trioctylphosphine (TOP).[17] To the best of our knowledge, most synthetic systems of Cu-based NPs with core-shell or alloyed structures are based on wet chemical reactions, which produce uniform NPs with precise control of size and morphology. However, many of these reactions have the disadvantages of multiple synthesis steps, necessary post-formation purification, and small-scale production limits.[18]

Previously, some of the authors reported on the mix-bake-wash process for the preparation and treatment of nanomaterials.[19] Herein, we report a structure-controllable and scalable one-pot synthesis of AgCu bimetallic NPs via this solventless mix-bake-wash approach. Small-sized bimetallic nanomaterials are obtained by heat treatment, using salt powder as a template. Moreover, the structural morphology of core-shell versus alloy formation can be controlled by tuning the annealing temperature. The size, structure, elemental distribution, and surface chemical identification of Ag@Cu core-shell and AgCu alloy NPs were characterized by HR-TEM, FE-SEM, EDX, HAADF-STEM, XRD, XPS, and CV measurement.

Scheme 1 Schematic of the procedure for preparing Ag-Cu NPs with different bimetallic nanostructures.

[a] *Program in Nano Science and Technology, Department of Transdisciplinary Studies, Graduate School of Convergence Science and Technology, Seoul National University, Seoul 151-742, Republic of Korea. E-mail: parkat9@snu.ac.kr; Fax: +82 31 888 9148*
[b] *Advanced Institutes of Convergence Technology, Seoul National University, Suwon 443-270, Republic of Korea.*
[c] *Center for Nanoparticle Research, Institute for Basic Science (IBS)*
† Electronic Supplementary Information (ESI) available: Digital photographs, additional SEM and TEM images. See DOI: 10.1039/x0xx00000x

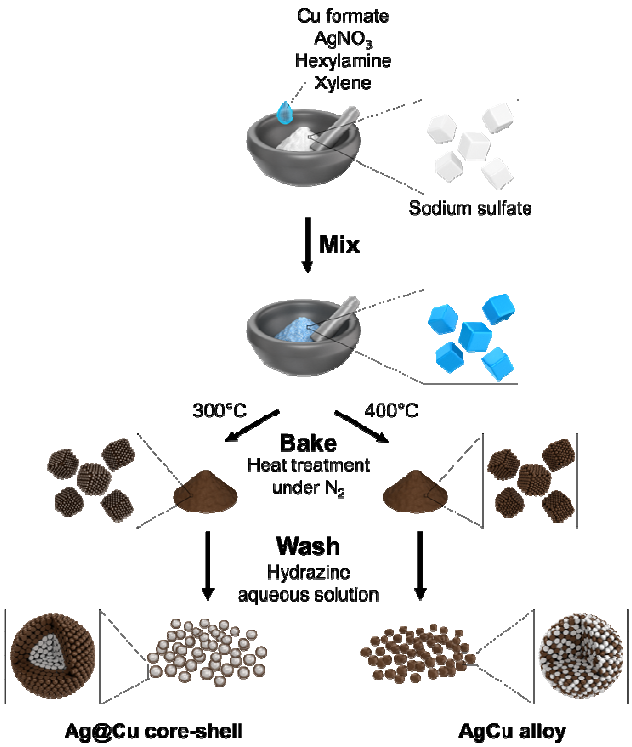

Scheme 1 Schematic of the procedure for preparing Ag-Cu NPs with different bimetallic nanostructures.

Experimental

Chemicals

Copper (II) formate tetrahydrate ($(HCO_2)_2Cu{\cdot}4H_2O$, 98%) and hexylamine ($CH_3(CH_2)_5NH_2$, 99%) were obtained from Alfa Aesar and Sigma-Aldrich, respectively. Silver nitrate ($AgNO_3$, 99.8%), xylene ($C_6H_4(CH_3)_2$, 99.5%), and sodium sulfate (Na_2SO_4, 98.5%) were purchased from Samchun Pure Chemical Co. Ltd, Korea. The sodium sulfate was processed by a grinder to obtain a homogeneous fine powder.

Synthesis of Ag@Cu core-shell NPs

In a typical synthesis, 0.675 g of copper (II) formate tetrahydrate (3 mmol) and 0.17 g of silver nitrate (1 mmol) were dissolved in 9 mL and 3 mL of a mixture of hexylamine/xylene (1:5 v/v), respectively. The two precursor solutions were mixed until homogeneous, and then mixed with 80 g of sodium sulfate fine powder using a mortar and pestle. The resulting powder was placed in a tube furnace with a temperature ramp of 3 °C min^{-1} to 300 °C under N_2 atmosphere and kept at 300 °C for 1 h. After cooling to room temperature, the product was purified with 0.1 M aqueous hydrazine solution at least five times to remove salts, and then redispersed in ethanol.

Synthesis of AgCu alloy NPs

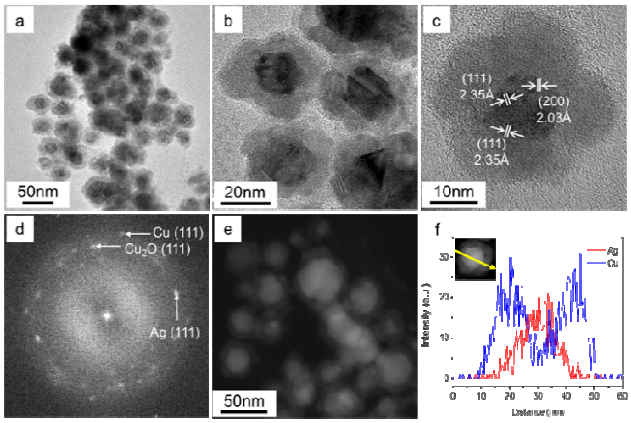

Fig. 1 Morphological and compositional characterization of Ag@Cu core-shell NPs: (a, b) TEM images, (c) HR-TEM image, (d) FFT diffraction pattern of (c), (e) HAADF-STEM image, and (f) corresponding EDX line-scanning profiles along the line in inset.

The synthesis of AgCu homogeneous alloy NPs was achieved by the same procedure. In order to obtain homogeneous alloy NPs, a higher temperature was required. The annealing temperature was increased to 400 °C instead of 300 °C.

Physiochemical characterization

The as-prepared AgCu bimetallic NPs were characterized by low- and high-resolution (HR) transmission electron microscopy (TEM) using a JEOL JEM-2100F instrument at an acceleration voltage of 120 kV, equipped with an energy-dispersive X-ray spectroscopy (EDX) detector. EDX spectra from a bimetallic NP were taken in high-angle annular dark-field scanning transmission electron microscopy (HAADF-STEM) mode. TEM samples were prepared by drop-casting the ethanolic suspension of the NPs onto a C-coated Ni grid and air-drying. Field-emission scanning electron microscopy (FE-SEM) imaging was carried out using a Hitachi S-4800 microscope with an accelerating voltage of 15 kV. X-ray diffraction (XRD) patterns were obtained with a Bruker D8 Advanced X-ray diffractometer. X-ray photoelectron spectroscopy (XPS) investigation was conducted in a KRATOS AXIS HSi spectrometer using an Mg Kα X-ray source.

Electrochemical characterization

Cyclic voltammetric (CV) measurement was performed with a Metrohm Autolab PGSTAT302N Potentiostat/Galvanostat using a three-electrode electrochemical system and 0.1 M KNO_3 as the electrolyte at room temperature. A Pt wire and Hg/HgO were used as the counter electrode and the reference electrode, respectively. The working electrode was a glassy carbon electrode with a 3 mm diameter. CV curves were recorded at a scanning rate of 100 mV s^{-1} within the potential range between -0.5 V and 0.8 V (vs. Hg/HgO).

Results and discussion

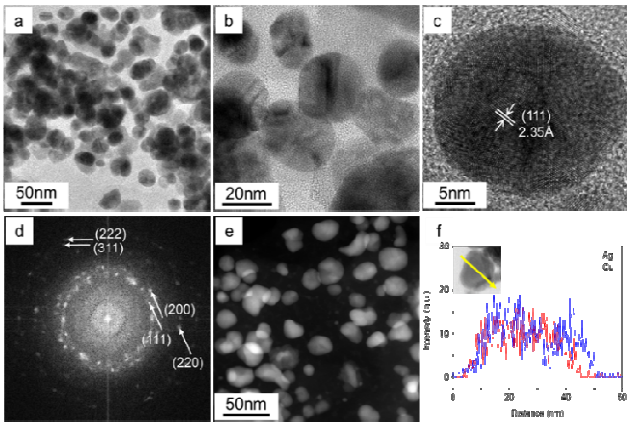

Fig. 2 Morphological and compositional characterization of AgCu alloy NPs: (a, b) TEM images, (c) HR-TEM image, (d) FFT diffraction pattern of (c), (e) HAADF-STEM image, and (f) the corresponding EDX line-scanning profiles along the line in inset.

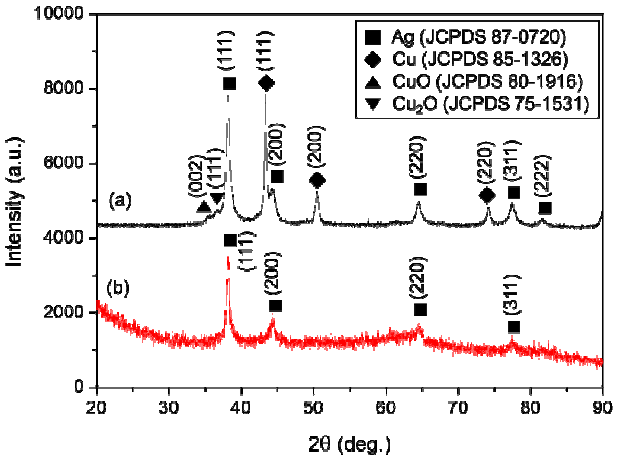

Fig. 3 XRD patterns of the synthesized (a) Ag@Cu core-shell NPs and (b) AgCu alloy NPs. The diffraction peaks ascribed to Ag, Cu, CuO, and Cu_2O are marked with the symbols ■, ◆, ▲, and ▼, respectively.

Controlled synthesis of Ag-Cu core-shell and alloy bimetallic nanoparticles

Scheme 1 illustrates the synthetic approach for preparing Ag-Cu bimetallic NPs by the solventless mix-bake-wash method. We synthesized two types of nanostructures: Ag@Cu hetero-structured core-shell and AgCu homogeneous alloy NPs. The first step in this synthesis was mixing salt powder with the precursor organic solution, which was prepared by dissolving Ag and Cu precursors in xylene using hexylamine as a phase transfer agent.[20] The mixture was heated at different temperatures to control the resulting NPs' structure under an inert N_2 atmosphere. When the reaction temperature was held at 150 °C, the initial blue color of the powder mixture began to change to red-brown, implying the formation of Cu NPs.[21] As the reaction temperature increased, the powder turned black-brown, suggesting a bimetallic complex between the Ag and Cu NPs.[22] In the final step, the synthesized NPs were obtained by washing and dissolving the salt powder in hydrazine aqueous solution, which also served to prevent oxidation of Cu.[15a,23]

Some typical morphologies of the Ag@Cu core-shell NPs obtained are shown in Fig. 1a-b. They often exhibit a flower-like shape; the average diameter of these NPs is 37.8 ± 8.3 nm with an average core size of 21.4 ± 5.9 nm and a shell thickness of 8.2 ± 2.1 nm. The core-shell nanostructure can be clearly distinguished in TEM and STEM images, due to the difference in electron penetration efficiency of Ag and Cu (Fig. 1a-c and e). HAADF-STEM imaging, in particular, shows the relative position of the elements within the nanomaterials due to the atomic number (Z)-based contrast.[24] In this case, it can be seen that the NPs are formed of faint shells on relatively brighter cores, indicating the formation of a core-shell nanostructure; that is, an Ag core (Z_{Ag} = 47) encircled by a Cu shell (Z_{Cu} = 29). Further detailed elemental and crystallographic analysis of core-shell NPs was obtained by EDX measurements, HR-TEM imaging, and fast Fourier transform (FFT) diffraction pattern observation. Fig. 1f shows the EDX line profiles through the center of a single Ag@Cu NP. As observed, the Ag signal is predominantly distributed in the core region, while the Cu signal is located in the outer region of the NP. A HR-TEM image of the core shows lattice fringes with *d* spacing of 2.35 Å and 2.03 Å, corresponding to the (111) and (200) planes of silver, respectively, revealing that the particle is polycrystalline with multiple crystal domains (Fig. 1c).[25] Meanwhile, the corresponding FFT diffraction pattern shows the coexistence of cuprous oxide (Cu_2O) with monometallic Cu and Ag phases (Fig. 1d).

In the synthesis, the ratio of Ag to Cu precursors was maintained and the heating temperature was increased to 400 °C to fabricate homogeneous alloyed NPs. Fig. 2a-b shows TEM images of AgCu alloy NPs with an average diameter of 27.7 ± 5.4 nm. Most of the particles display close to spherical morphology. HR-TEM shows a single nanostructure with a fringe spacing of 2.35 Å, corresponding to the interplanar distance of (111) planes in face-centered cubic (fcc) Ag. The corresponding FFT diffraction pattern is also consistent with fcc Ag, suggesting that the AgCu alloy NPs have a crystal structure similar to pure Ag (Fig. 2c-d).[25b,26] AgCu alloy NPs also have differently oriented domains within a single NP, implying that the prepared nanoalloys have a polycrystalline structure. To provide definitive evidence of the alloy structure of the AgCu NPs, HAADF-STEM imaging and EDX line-scanning were performed. HAADF-STEM image shows no obvious contrast change, unlike the core-shell segregation of Ag and Cu, while EDX line-scan profiles show that Ag and Cu coexist and almost completely overlap, indicating the existence of Ag and Cu within a single nanostructure and the formation of an alloy (Fig. 2e-f).

Structural and chemical characterization

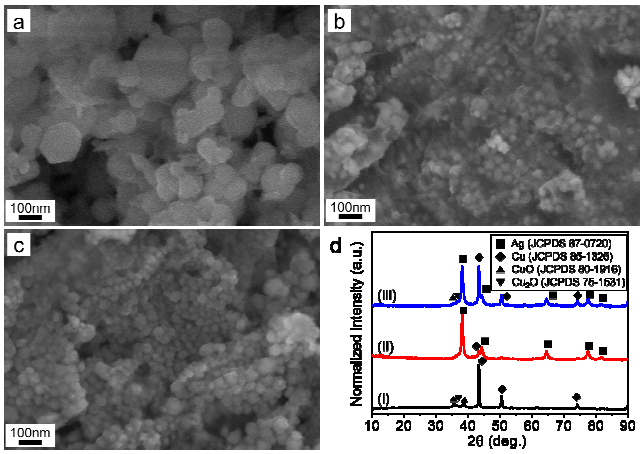

Fig. 4 SEM images of pure Cu NPs (a), Ag@Cu core-shell NPs with Ag to Cu molar ratios of 1:1 (b) and 1:3 (c). (d) Comparison of XRD patterns of pure Cu (I), Ag@Cu core-shell NPs with Ag to Cu molar ratios of 1:1 (II) and 1:3 (III). The diffraction peaks ascribing to Ag, Cu, CuO, and Cu_2O are marked with the symbols ■, ◆, ▲, and ▼, respectively.

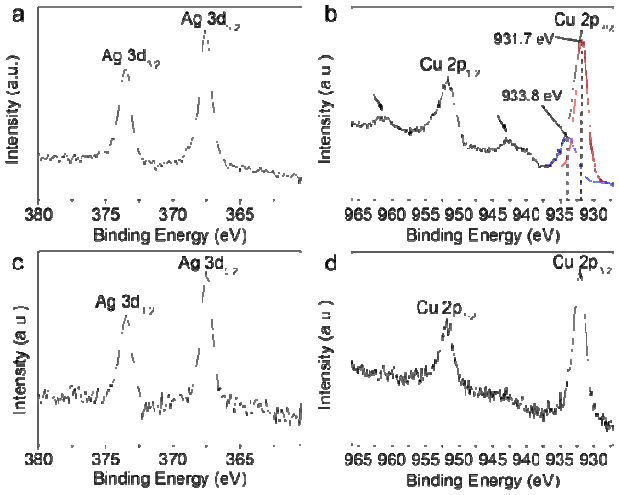

Fig. 5 XPS patterns in the binding energy range of (a, c) Ag 3d and (b, d) Cu 2p from (a, b) Ag@Cu core-shell NPs and (c, d) AgCu alloy NPs, respectively.

The XRD patterns of bimetallic Ag@Cu core-shell and AgCu alloy NPs are shown in Fig. 3. The diffraction peaks of the Ag@Cu core-shell NPs appear to consist of sets of peaks associated with (i) Ag (JCPDS 87-0720), (ii) Cu (JCPDS 85-1326), and (iii) copper oxides (CuO, JCPDS 80-1916; Cu_2O, JCPDS 75-1531), suggesting the segregation of Cu and Ag with fcc crystal structures and the existence of low levels of cuprous or cupric oxide, in agreement with the HR-TEM and FFT results (Fig. 1c-d, Fig. 3a). The XRD pattern of the AgCu alloy NPs shows four peaks at 2θ values of 38.1, 44.2, 64.4, and 77.8°. These peaks were indexed as the (111), (200), (220), and (311) planes of Ag's fcc structure, indicating that the as-prepared AgCu alloy NPs have the same crystal structure as Ag.[15b,27] In addition, no peaks from copper oxides were detected.

In order to further understand the formation of small-sized Ag@Cu core-shell NPs, the detailed molar ratio-dependent evolution of morphology and crystal structure were investigated by FE-SEM and XRD, as shown in Fig. 4. When only copper (II) formate tetrahydrate was applied as a Cu precursor and heated to 300 °C, the product was large-sized spherical Cu NPs with mean diameter of about 130 nm (Fig.4a). These NPs had an fcc structure including trace copper oxide (Fig. 4d). Once silver nitrate (Ag precursor) was included in the reaction mixture, a significant decrease in particle size (ca. 30–40 nm) was observed (Fig. 4b, c). The core-shell structure can be clearly observed in Fig. S2, and their diffraction peaks indicates the presence of both Ag and Cu, with trace copper oxides. It was confirmed that the peak intensity of Cu increases with an increase in the molar ratio of Ag to Cu from 1:1 to 1:3, caused by a difference in the shell thickness of Cu. We observed that Ag plays an important role for the formation of small-sized Ag-Cu bimetallic NPs.

XPS was performed to further investigate the surface chemical compositions and the valence states of Cu and Ag in the Ag@Cu core-shell and AgCu alloy NPs (Fig. 5). Fig. 5a and c show that the Ag 3d spectra contains two sets of spin-orbit split peaks at 373.6 eV and 367.6 eV, which can be attributed to the binding energies of Ag $3d_{3/2}$ and Ag $3d_{5/2}$, respectively. This confirms that Ag in core-shell NPs and alloy NPs exists as metallic Ag^0.[28] In the case of Cu in Ag@Cu core-shell NPs, as shown in Fig. 5b, the major peaks appear at 951.6 eV for Cu $2p_{1/2}$ and 931.8 eV for Cu $2p_{3/2}$. The Cu $2p_{3/2}$ peak can be

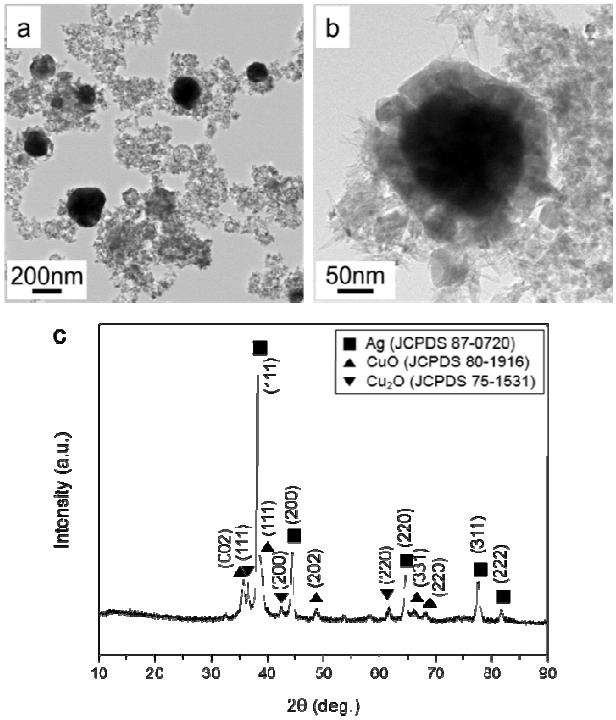

Fig. 6 (a, b) TEM images and (c) XRD patterns of Ag-Cu_xO (x=1, 2) hybrid NPs prepared under the same reaction conditions for Ag@Cu core-shell NPs, but without salt powders.

further divided into two peaks at 933.8 eV and 931.7 eV, corresponding to the formation of Cu^{2+} and Cu^0, respectively.[28-29] Furthermore, satellite peaks at 961.6 eV and 943.1 eV, located at higher binding energies than those of the major peaks, reveals more clearly that Ag@Cu core-shell NPs, reacted at lower temperature, contain Cu^{2+} species. However, the peak intensity of Cu^{2+} at 933.8 eV is lower than that of Cu^0 at 931.7 eV, implying a smaller quantity of Cu^{2+} formed, compared to the amount of Cu^0. In the case of Cu in AgCu alloy NPs, the spin-orbit split Cu peaks at 951.9 eV and 932.0 eV agree with the binding energies of Cu $2p_{1/2}$ and Cu $2p_{3/2}$ of metallic Cu^0, respectively; no oxide species were detected.[28,29a,30] The above information provides sufficient evidence that AgCu alloy NPs existed fully in the metallic state, whereas some Cu atoms in the Ag@Cu core-shell NPs experienced oxidation.

Investigation of the effect of salt powder on the synthesis of Ag-Cu bimetallic nanoparticles

To check the ability of the solventless mix-bake-wash method to control the size and morphology of bimetallic NPs, an additional experiment was performed. The same reaction conditions used to create Ag@Cu core-shell NPs were used, without salt powder. Instead of forming core-shell-structured bimetallic NPs, much larger spherical Ag NPs (>150 nm) and amorphous copper oxide were generated (Fig. 6a-b, S3). Although some core-shell NPs were observed, the shell structure is not Cu metal but copper oxide species, confirmed by XRD measurements (Fig. 6b-c). Moreover, this wet chemical method had a maximum reaction temperature of 300 °C because of the liquid solvent, whereas the temperature in the solventless method could easily be raised to 400 °C or higher for alloying of Ag and Cu.

As can be seen from these results, the solventless mix-bake-wash approach in this work has several advantages. First, this strategy is attractive and practical to synthesize alloy NPs because salt powder has a very wide temperature window from 200 to 600 °C. In addition, the salt powder serves as a template to prevent aggregation of NPs during synthesis, instead of capping agents in a wet chemical method. Second, the structural morphology of core-shell and alloy can be easily controlled by tuning the annealing temperature. Lastly, the proposed synthetic strategy can be readily scalable for nanomaterial fabrication on an industrial scale.

Electrochemical analysis of Ag-Cu bimetallic nanoparticles

The surface structure of Ag-Cu bimetallic NPs is one of the key factors affecting their catalytic and electrical performance.[16a,31] CV is an efficacious method to study surface reactions of metals.[33] We conducted CV measurements to investigate the chemical identification of the surface species. Fig. 7 shows the CV curves of Ag@Cu core-shell and AgCu alloy NPs with equal weight in 0.1 M KNO_3 at a potential range of -0.5 ~ 0.8 V vs. Hg/HgO. Typical two anodic peaks corresponding to the oxidation of Cu from Ag@Cu core-shell NPs were observed at 0.111 V and 0.239 V (vs. Hg/HgO), which can be attributed to the dissolution of Cu.[31] For AgCu alloy NPs, there is one oxidation peak in the forward scan and the peak current was significantly decreased as compared to that of Ag@Cu core-shell NPs. This analysis supports the observation that the surface of AgCu alloy NPs are composed by relatively low Cu content, in good agreement with TEM and EDX results, and the oxidation resistance is enhanced by alloying.

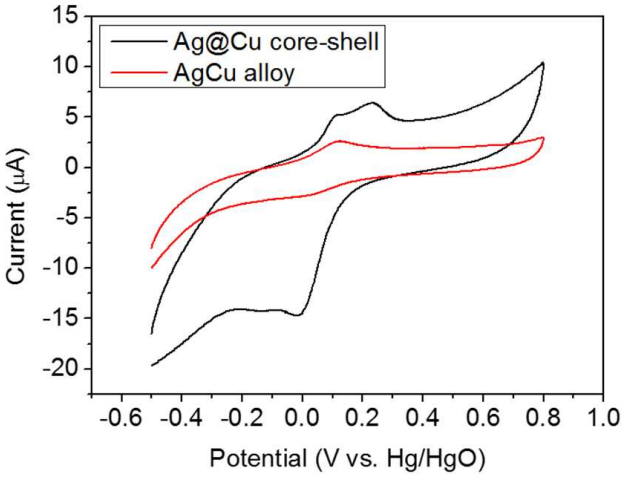

Fig. 7 Cyclic voltammogram curves of Ag@Cu core-shell NPs (black line) and AgCu alloy NPs (red line) recorded in 0.1 M KNO_3. Scan rate: 100 mV s^{-1}.

Conclusions

A solventless mix-bake-wash method using salt powder was developed to fabricate uniform Ag-Cu core-shell and alloy bimetallic NPs. The feature of our synthetic strategy that distinguishes it from those reported earlier is the use of salt powder, which serves as a template to prevent the aggregation of NPs during synthesis. The as-synthesized Ag-Cu bimetallic NPs have diameters in the range of 30–40 nm. The structures of the NPs can be tuned by the reaction temperature, allowing for selection between hetero-structured core-shell NPs and homogeneous alloys. Ag@Cu core-shell NPs show a flower-like shape and consist of fcc metal Ag and Cu, with trace levels of copper oxides. AgCu nanoalloys show a single phase with fcc structure similar to Ag, containing no copper oxides. The results of CV indicated that the surface of AgCu alloy NPs are composed by relatively low Cu content and the oxidation resistance is enhanced by alloying. The methodology reported here has distinct advantages: 1) The lack of solvent makes it possible to synthesize alloys in a wide temperature window. 2) The structural morphology of core-shell versus alloy can be tuned by adjusting only the annealing temperature. 3) The proposed synthesis strategy is easily scalable for large-scale production. We believe that this approach can be extended to produce other important bimetallic NPs, such as CuAu and CuPt. These structure-controlled bimetallic NPs may be found to be useful in electronics, biomedical research, and catalysis.

Acknowledgements

This work was supported by Nano Material Technology Development Program (2014M3A7B6020163) of MSIP/NRF and by the Center for Integrated Smart Sensors funded by the Ministry of Science, ICT and Future Planning, Republic of Korea, as Global Frontier Project (CISS-012M3A6A6054186). This work was also supported by Project Code (IBS-R006-D1).

Notes and references

1 *(a)* D. Wang and Y. Li, *Adv. Mater.*, 2011, **23**, 1044-1060; *(b)* C. Burda, X. Chen, R. Narayanan and M. A. El-Sayed, *Chem. Rev.*, 2005, **105**, 1025-1102; *(c)* S. Alayoglu, A. U. Nilekar, M. Mavrikakis and B. Eichhorn, *Nat. Mater.*, 2008, **7**, 333-338; *(d)* S. U. Son, Y. Jang, J. Park, H. B. Na, H. M. Park, H. J. Yun, J. Lee and T. Hyeon, *J. Am. Chem. Soc.*, 2004, **126**, 5026-5027; *(e)* D. Sun, V. Mazumder, O. Metin and S. Sun, *ACS nano*, 2011, **5**, 6458-6464; *(f)* D. Wang, Q. Peng and Y. Li, *Nano Res.*, 2010, **3**, 574-580.

2 *(a)* O. Chen, J. Zhao, V. P. Chauhan, J. Cui, C. Wong, D. K. Harris, H. Wei, H.-S. Han, D. Fukumura, R. K. Jain and M. G. Bawendi, *Nat. Mater.*, 2013, **12**, 445-451; *(b)* J. P. Wilcoxon and P. P. Provencio, *J. Am. Chem. Soc.*, 2004, **126**, 6402-6408; *(c)* L. Wang, C. Clavero, Z. Huba, K. J. Carroll, E. E. Carpenter, D. Gu and R. A. Lukaszew, *Nano Lett.*, 2011, **11**, 1237-1240; *(d)* R. Ferrando, J. Jellinek and R. L. Johnston, *Chem. Rev.*, 2008, **108**, 845-910.

3 *(a)* D. A. Bussian, S. A. Crooker, M. Yin, M. Brynda, A. L. Efros and V. I. Klimov, *Nat. Mater.*, 2008, **8**, 35-40; *(b)* X. Wei, R. Zhou, W. Lefebvre, K. He, D. Le Roy, R. Skomski, X. Li, J. E. Shield, M. J. Kramer, S. Chen, X. C. Zeng and D. J. Sellmyer, *Nano Lett.*, 2014, **14**, 1362-1368; *(c)* J. F. Bondi, R. Misra, X. Ke, I. T. Sines, P. Schiffer and R. E. Schaak, *Chem. Mater.*, 2010, **22**, 3988-3994; *(d)* A. Demortière and C. Petit, *Langmuir*, 2007, **23**, 8575-8584.

4 *(a)* N. L. Rosi and C. A. Mirkin, *Chem. Rev.*, 2005, **105**, 1547-1562; *(b)* F. Wang, R. Deng, J. Wang, Q. Wang, Y. Han, H. Zhu, X. Chen and X. Liu, *Nat. Mater.*, 2011, **10**, 968-973; *(c)* J.-M. Nam, S. I. Stoeva and C. A. Mirkin, *J. Am. Chem. Soc.*, 2004, **126**, 5932-5933.

5 H. Kobayashi, M. Yamauchi, H. Kitagawa, Y. Kubota, K. Kato and M. Takata, *J. Am. Chem. Soc.*, 2010, **132**, 5576-5577.

6 *(a)* J.-P. Lee, D. Chen, X. Li, S. Yoo, L. A. Bottomley, M. A. El-Sayed, S. Park and M. Liu, *Nanoscale*, 2013, **5**, 11620-11624; *(b)* C. M. Andolina, A. C. Dewar, A. M. Smith, L. E. Marbella, M. J. Hartmann and J. E. Millstone, *J. Am. Chem. Soc.*, 2013, **135**, 5266-5269; *(c)* W.-Y. Ko, J.-W. Su, C.-H. Guo and K.-J. Lin, *Carbon*, 2012, **50**, 2244-2251.

7 *(a)* S. Sun, C. Murray, D. Weller, L. Folks and A. Moser, *Science*, 2000, **287**, 1989-1992; *(b)* T. Hyeon, *Chem. Commun.*, 2003, 927-934; *(c)* B. Y. Kim, I.-B. Shim, Z. O. Araci, S. S. Saavedra, O. L. Monti, N. R. Armstrong, R. Sahoo, D. N. Srivastava and J. Pyun, *J. Am. Chem. Soc.*, 2010, **132**, 3234-3235.

8 *(a)* Y. Mizukoshi, T. Fujimoto, Y. Nagata, R. Oshima and Y. Maeda, *J. Phys. Chem. B*, 2000, **104**, 6028-6032; *(b)* S. Anandan, F. Grieser and M. Ashokkumar, *J. Phys. Chem. C*, 2008, **112**, 15102-15105.

9 *(a)* Y. Song, Y. Ma, Y. Wang, J. Di and Y. Tu, *Electrochim. Acta*, 2010, **55**, 4909-4914; *(b)* U. Kolb, S. A. Quaiser, M. Winter and M. T. Reetz, *Chem. Mater.*, 1996, **8**, 1889-1894.

10 *(a)* O. Pena, U. Pal, L. Rodríguez-Fernández, H. G. Silva-Pereyra, V. Rodríguez-Iglesias, J. C. Cheang-Wong, J. Arenas-Alatorre and A. Oliver, *J. Phys. Chem. C*, 2009, **113**, 2296-2300; *(b)* G. Mattei, C. Maurizio, P. Mazzoldi, F. D'Acapito, G. Battaglin, E. Cattaruzza, C. de Julián Fernández and C. Sada, *Phys. Rev. B*, 2005, **71**, 195418.

11 *(a)* R. Harpeness and A. Gedanken, *Langmuir*, 2004, **20**, 3431-3434; *(b)* Z. Liu, J. Y. Lee, W. Chen, M. Han and L. M. Gan, *Langmuir*, 2004, **20**, 181-187.

12 *(a)* X. Teng and H. Yang, *J. Am. Chem. Soc.*, 2003, **125**, 14559-14563; *(b)* B. Nakhjavan, M. N. Tahir, F. Natalio, H. Gao, K. Schneider, T. Schladt, I. Ament, R. Branscheid, S. Weber, U. Kolb, C. Sonnichsen, L. M. Schreiber and W. Tremel, *J. Mater. Chem.*, 2011, **21**, 8605-8611.

13 *(a)* F. Tao, M. E. Grass, Y. Zhang, D. R. Butcher, J. R. Renzas, Z. Liu, J. Y. Chung, B. S. Mun, M. Salmeron and G. A. Somorjai, *Science*, 2008, **322**, 932-934; *(b)* J.-M. Yan, X.-B. Zhang, S. Han, H. Shioyama and Q. Xu, *J. Power Sources*, 2009, **194**, 478-481; *(c)* H. M. Chen, C. F. Hsin, P. Y. Chen, R.-S. Liu, S.-F. Hu, C.-Y. Huang, J.-F. Lee and L.-Y. Jang, *J. Am. Chem. Soc.*, 2009, **131**, 15794-15801; *(d)* K. Shin, D. H. Kim and H. M. Lee, *ChemSusChem*, 2013, **6**, 1044-1049.

14 *(a)* Y. Sugano, Y. Shiraishi, D. Tsukamoto, S. Ichikawa, S. Tanaka and T. Hirai, *Angew. Chem.*, 2013, **125**, 5403-5407; *(b)* S. Piccinin, S. Zafeiratos, C. Stampfl, T. W. Hansen, M. Hävecker, D. Teschner, V. I. Bukhtiyarov, F. Girgsdies, A. Knop-Gericke, R. Schlögl and M. Scheffler, *Phys. Rev. Lett.*, 2010, **104**, 035503; *(c)* J. Yang, L. L. Chng, X. Yang, X. Chen and J. Y. Ying, *Chem. Commun.*, 2014, **50**, 1141-1143; *(d)* W. Wu, M. Lei, S. Yang, L. Zhou, L. Liu, X. Xiao, C. Jiang and V. A. L. Roy, *J. Mater. Chem. A*, 2015, **3**, 3450-3455; *(e)* J. Liu, Q. Wu, F. Huang, H. Zhang, S. Xu, W. Huang and Z. Li, *RSC Adv.*, 2013, **3**, 14312-14321.

15 *(a)* M. Taner, N. Sayar, I. G. Yulug and S. Suzer, *J. Mater. Chem.*, 2011, **21**, 13150-13154; *(b)* M. Valodkar, S. Modi, A. Pal and S. Thakore, *Mater. Res. Bull.*, 2011, **46**, 384-389.

16 *(a)* M. Grouchko, A. Kamyshny and S. Magdassi, *J. Mater. Chem.*, 2009, **19**, 3057-3062; *(b)* S. J. Kim, E. A. Stach and C. A. Handwerker, *Appl. Phys. Lett.*, 2010, **96**, 144101; *(c)* C. K. Kim, G.-J. Lee, M. K. Lee and C. K. Rhee, *Powder Technol.*, 2014, **263**, 1-6.

17 V. Mazumder, M. Chi, M. N. Mankin, Y. Liu, O. n. Metin, D. Sun, K. L. More and S. Sun, *Nano Lett.*, 2012, **12**, 1102-1106.

18 T. Yan, X. Zhong, A. E. Rider, Y. Lu, S. A. Furman and K. Ostrikov, *Chem. Commun.*, 2014, **50**, 3144-3147.

19 *(a)* B. Jang, M. Park, O. B. Chae, S. Park, Y. Kim, S. M. Oh, Y. Piao and T. Hyeon, *J. Am. Chem. Soc.*, 2012, **134**, 15010-15015; *(b)* Y. I. Park, Y. Piao, N. Lee, B. Yoo, B. H. Kim, S. H. Choi and T. Hyeon, *J. Mater. Chem.*, 2011, **21**, 11472-11477; *(c)* Y. Piao, J. Kim, H. B. Na, D. Kim, J. S. Baek, M. K. Ko, J. H. Lee, M. Shokouhimehr and T. Hyeon, *Nat. Mater.*, 2008, **7**, 242-247.

20 L. Liu and T. L. Kelly, *Langmuir*, 2013, **29**, 7052-7060.

21 M. Jin, G. He, H. Zhang, J. Zeng, Z. Xie and Y. Xia, *Angew. Chem. Int. Ed.*, 2011, **50**, 10560-10564.

22 A. K. Sra and R. E. Schaak, *J. Am. Chem. Soc.*, 2004, **126**, 6667-6672.

23 S. Magdassi, M. Grouchko and A. Kamyshny, *Materials*, 2010, **3**, 4626-4638.

24 *(a)* S. J. Pennycook and D. E. Jesson, *Ultramicroscopy*, 1991, **37**, 14-38; *(b)* S. J. Pennycook and D. E. Jesson, *Acta Metall. Mater.*, 1992, **40**, S149-S159; *(c)* A. López-Ortega, M. Estrader, G. Salazar-Alvarez, A. G. Roca and J. Nogués, *Phys. Rep.*, 2015, **553**, 1-32.

25 *(a)* T. Bai, J. Sun, R. Che, L. Xu, C. Yin, Z. Guo and N. Gu, *ACS Appl. Mater. Interfaces*, 2014, **6**, 3331-3340; *(b)* M. Chen, C. Wang, X. Wei and G. Diao, *J. Phys. Chem. C*, 2013, **117**, 13593-13601.

26 T. I. Yang, R. N. C. Brown, L. C. Kempel and P. Kofinas, *Nanotechnology*, 2011, **22**, 105601.

27 *(a)* Y. Lei, F. Chen, B. Huang and Z. Liu, *Mater. Res. Express*, 2014, **1**, 015031; *(b)* C.-H. Huang, H. P. Wang, J.-E. Chang and E. M. Eyring, *Chem. Commun.*, 2009, 4663-4665.
28 R. Morrish and A. J. Muscat, *Chem. Mater.*, 2009, **21**, 3865-3870.
29 *(a)* H.-B. Noh, K.-S. Lee, P. Chandra, M.-S. Won and Y.-B. Shim, *Electrochim. Acta*, 2012, **61**, 36-43; *(b)* V. Bansal, H. Jani, J. Du Plessis, P. J. Coloe and S. K. Bhargava, *Adv. Mater.*, 2008, **20**, 717-723.
30 *(a)* D.-H. Shin, S. Woo, H. Yem, M. Cha, S. Cho, M. Kang, S. Jeong, Y. Kim, K. Kang and Y. Piao, *ACS Appl. Mater. Interfaces*, 2014, **6**, 3312-3319; *(b)* Z. Yin, C. Lee, S. Cho, J. Yoo, Y. Piao and Y. S. Kim, *Small*, 2014, **10**, 5047-5052.
31 A. Holewinski, J.-C. Idrobo and S. Linic, *Nat. Chem.*, 2014, **6**, 828-834.
32 T. Zhang, R. Yuan, Y. Chai, W. Li and S. Ling, *Sensors*, 2008, **8**, 5141-5152.
33. *(a)* T. A. Aljohani, B. E. Hayden, Electrochim. Acta, 2013, 111, 930–936; *(b)* D. Chen, N. Jin, W. Chen, L. Wang, S. Zhao and D. Luo, Surf. Coat. Technol., 2014, 254, 440–446.

Table of contents

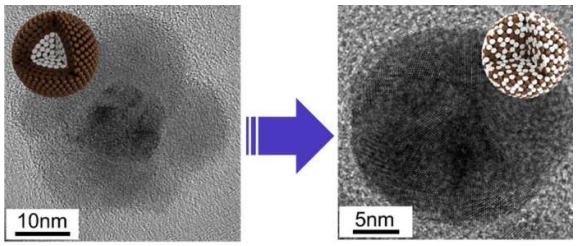

A solventless mix-bake-wash method using salt powder was developed to fabricate uniform Ag-Cu core-shell and alloy bimetallic nanoparticles.